

INFLUENCE OF MULTIPLICITY ON PROPERTIES OF nd_x ($x= 6, 7$ and 8) HALIDE TRANSITION METAL(II) COMPLEXES OF GLYOXIME LIGAND IN GAS PHASE AND AQUEOUS SOLUTION: COMPUTATIONAL ASSESSMENT.

DJENDO MAZIA SUZANE LEONIE (✉ djendoleonie83@gmail.com)

University of Douala

MOTO ONGAGNA JEAN (✉ jean.monfils@yahoo.fr)

University of Douala

ADJIEUFACK ABEL IDRICE (✉ adjieufack21@gmail.com)

University of Yaoundé I

LISSOUCK Daniel (✉ lissouckdaniel@yahoo.com)

University of Douala

NDOM JEAN CLAUDE (✉ ndomjefr@yahoo.fr)

University of Douala

BIKELE MAMA DÉsirÉ (✉ bikelemama@yahoo.fr)

University of Douala

Research Article

Keywords: nd_x ($x= 6,7$ and 8) transition metal, QMAIM, Charge Decomposition Analysis, Energy Decomposition Analysis and DFT.

DOI: <https://doi.org/10.21203/rs.3.rs-2431811/v1>

License: © ⓘ This work is licensed under a Creative Commons Attribution 4.0 International License.

[Read Full License](#)

INFLUENCE OF MULTIPLICITY ON PROPERTIES OF nd^x (x= 6, 7 and 8) HALIDE TRANSITION METAL(II) COMPLEXES OF GLYOXIME LIGAND IN GAS PHASE AND AQUEOUS SOLUTION: COMPUTATIONAL ASSESSMENT.

DJENDO MAZIA SUZANE LEONIE^a, MOTO ONGAGNA JEAN^a, ADJIEUFACK ABEL IDRICE^b, LISSOUCK Daniel^c, NDOM JEAN CLAUDE^a, BIKELE MAMA DÉSIRÉ^{a*}

^a Department of Chemistry, Faculty of Science, University of Douala, P.O. Box 24157, Douala, Cameroon.

^b Physical and Theoretical Chemistry Laboratory, University of Yaoundé I, P.O. Box 812 Yaoundé, Cameroon.

^c Department of Physics, Faculty of Science, University of Douala, P.O. Box 24157, Douala, Cameroon.

* Corresponding author contact details:

Pr. BIKELE MAMA Désiré
Associate Professor
Computational and Theoretical Chemistry Expert
Head of the Computational and Theoretical Chemistry Unit
Department of Chemistry/University of Douala, Cameroon.
Tel: +237 6 79 27 85 19/+237 6 93 01 77 50
Email: Bikelemama@yahoo.fr

ABSTRACT

The present paper has been focused on the ability of the glyoxime ligand to chelate to the $[MX_2]$ inorganic moieties in which M and X refer respectively to nd^x transition metal (x = 6, 7 and 8) and halogenated ligand (X = Br or Cl). The geometry optimizations at B3LYP/GEN level (LanL2DZ and 6-311+G (d,p) respectively for nd^x transition metals (as well as halogen atoms) and for others atoms) have integrated the alteration of the multiplicity in each study media (gas phase and water). The passage from the fourth period transition metals to the sixth period ones enhances the reactivity of the complexes obtained regardless in gas phase. The metal-nitrogen bonds within higher multiplicity nd^x (x=7,8) transition metal complexes are most unstable in both media. The [glyoxime ligand] ... $[MX_2]$ interaction strength increases in the following order: $Fe^{2+} < Co^{2+} < Ni^{2+}$ (**3d series**); $Pd^{2+} < Rh^{2+} < Ru^{2+}$ (**4d series**) and $Pt^{2+} < Ir^{2+} < Os^{2+}$ (**5d series**). For lower multiplicity bromide complexes exclusively, the enhancement of the donor character of the organic glyoxime ligand is promoted by its solvation except for nd^6 transition metal complexes.

Keywords: nd^x ($x= 6,7$ and 8) transition metal, QMAIM, Charge Decomposition Analysis, Energy Decomposition Analysis and DFT.

1-INTRODUCTION

Vic glyoxime ligands possess many applications in many fields (industries, agriculture and medicine) [1-4]. Dichloroglyoxime ligand exhibits a sensitive activity against (gram-positive and gram-negative) bacteria [5]. The investigation on new antibacterial bioactive justifies the enrichment of quinoline compound by glyoxime [6]. Due to their importance, glyoxime ligands are extensively used in many areas in chemistry. Currently, considered as model molecules to mimic the reduction of the vitamin B₁₂ [7], vic-dioxime ligands are amphoteric. This is due to the simultaneous presence of mildly hydroxyl group and slightly basic nitrogen atom. Numerous biological and semiconducting properties[8, 9] justify the great attention given to their metal complexes. The remarkable usage of the nickel vic-dioxime in voltammetry, thermal decomposition and spectrophotometry is worthy of notice [10-11]. The outstanding stability observed strengthened by the formation of hydrogen bonds is a result of the planar configuration of complexes. For an adequate analysis of the stability of these complexes, the isomeric parameters of vic-dioxime ligands depending on the symmetry of the molecules must be integrated. For instance, three structural suggestions (syn, anti and amphi) need to be taken into account for a scrutiny of symmetrical molecular structures. In ordinary way, the stability follows the following decreasing order: anti > amphi > syn configuration. Experimentally, a relationship has been established between two parameters: the colour of the complexes synthesized and the configuration of vic-dioxime ligand [11-12]. For example, oxime ligands (in the anti-configuration) yield brightly coloured complexes with nickel and others transition metal(TM) ions. With nickel ions particularly, complexes formed are blood red. Although, the numerous experimental works devoted to vic-oxime complexes, the explanation on this relationship between the colour of complexes and the configuration of vic-dioxime is still lacking. Fortunately, the computational chemistry tools can be used to overcome such an experimental limitation. But, the careful survey of the computational literature displayed few researches on this point [13-14]. In sake of the continuation, structural, spectral and thermodynamic properties of 3rd row transition metal (II) chloride complexes of glyoxime and its derivatives were investigated by the mean of computational tools (DFT and TD-DFT) [15]. Higher affinity of these ligands towards Ni (II) and Fe (II) and the thermodynamical feasibility of all complex reactions have been revealed. In the same vein, an extension of this analysis focused on chelation of divalent d^8 transition metal (II)

cation to dioxime ligands highlights the high ability of the latter to eliminate the agents in solution[16]. In the present works, we have investigated the coordination ability of divalent (nd^6 , nd^7 and nd^8) TM cations to chelate these ligands. This choice of divalent transition metal(II) cations is guided by the previous experimental investigation on oximes as spectrophotometric reagents[17]. For sake of simplicity, the dimethylglyoxime ligand is the main focus of our interest. This choice is practically motivated by its wide capacity to capture heavy metals from wastewater using the dimethylglyoxime ligand[18]. But, the accurate range of heavy metals caught by this ligand remains unknown. The depollution tests requires a comparative grid of the stability of the complexes formed which is not regrettably established. The variation of this stability provoked by the electronic excitation following possible solar exposure is not integrated in any experimental analysis. In this paper, we have focused exclusively on the influence of this excitation on the geometrical and thermodynamic parameters by means of the multiplicity variation of the formed complexes. More accurately, the influence of spin multiplicity states on the geometrical, thermodynamic and bonding properties has been scrutinized in two media (gas phase and water). The electronic and other properties of these complexes have been examined in other forthcoming studies.

2-COMPUTATIONAL DETAILS

The geometry optimization (without any symmetry constraints) of each structure of the molecular library has been done using the Gaussian 09W program [19]. They have been always followed by a frequency calculation. B3LYP functional chosen has been associated to a generic basis set (GEN: LanL2DZ for nd^x ($x= 6,7$ and 8) transition metals (also for halogen atoms (Br and Cl))) and polarized and diffuse triple Pople basis set (6-311++G(d,p)). Because of the lack of experimental data, the reliability of geometry prediction has not been done by adding the Grimmes's dispersion correction (GD3) to the geometry optimization constraints[20]. The complexation thermodynamic parameters denoted ΔZ ($Z = E$ (total energies), H (enthalpies) and G (free energies) have been estimated according to the equation (1):

$$\Delta Z = Z_{[MLX_2]} - (Z_L + Z_{M^{2+}} + 2Z_{X^-}) \quad (1)$$

The species symbolized by $[MLX_2]$ (complex formed), L (glyoxime ligand), M^{2+} (divalent nd^x ($x = 6,7$ and 8) TM cation) and X^- halogen anion (Cl^- and Br^-) are involved in the formation of complexe (2):



Through the QTAIM (quantum theory of atoms in molecules) approach[21] implemented in the Multiwfn program [22], the M...N and M...X interactions have been explored. For this purpose, the local kinetic electron energy density (3) and the potential energy density (4) respectively denoted $G(\mathbf{r})$ and $v(\mathbf{r})$ were used. These two main descriptors depend on two factors: the electron density ($\rho(\mathbf{r})$) and Laplacian at bond critical points ($\nabla^2\rho(\mathbf{r})$).

$$G(\mathbf{r}) = \frac{3}{10} (3\pi)^{2/3} \rho(\mathbf{r})^{5/3} + \frac{1}{6} \nabla^2 \rho(\mathbf{r}) \quad (3)$$

$$v(\mathbf{r}) = \frac{\hbar^2}{4m} \nabla^2 \rho(\mathbf{r}) - 2G(\mathbf{r}) \quad (4)$$

The sign of Laplacian reveals the nature of the interactions: covalent ($\nabla^2\rho(\mathbf{r}) < 0$) and electrostatic ($\nabla^2\rho(\mathbf{r}) > 0$) interactions. For further information on this nature, the ratio ($-G(\mathbf{r})/v(\mathbf{r})$) may be another topological tool to specify the interaction: non-covalent (the ratio greater than 1) and partially covalent (the ratio between 0.5 and 1) interactions. By combining of the sign of Laplacian to the value of the said ratio, the detection of intermediate ($-G(\mathbf{r})/v(\mathbf{r}) < 1$ and $\nabla^2\rho(\mathbf{r}) < 0$) and closed shell ($-G(\mathbf{r})/v(\mathbf{r}) > 1$ and $\nabla^2\rho(\mathbf{r}) < 0$)

interactions can be done. An another approach to examine the stability of the metal-ligand interaction has been performed by means of metal ion affinity estimation (MIA). The choice of the B3LYP functional for the said analysis lies on its ability to produce results significantly closer to the experimental ones [23-24]. The MIA (negative of the enthalpy during the formation process (2) of the [MLX₂] complexes) is defined according to equation (5) :

$$MIA = -[E_{el}([MLX_2]) - 2E_{el}(X^-) - E_{el}(L) - E_{el}(M^{2+})] + [E_{vib}([MLX_2]) - E_{vib}(L)] \quad (5)$$

The electronic energy (E_{el}) results from a calculation of the SCF. The search for vibrational frequencies allows the prediction of the vibrational contribution (E_{vib}) which includes the zero point energy and the temperature correction from 0 to 298 K [23]. Further quantitative information on intramolecular interactions [L]...[MX₂] was calculated through an energy decomposition (EDA) [24-25] in term of interaction energy (6) denoted ΔE_{int} between the two fragments involved:

$$\Delta E_{int} = \Delta E_{elstat} + \Delta E_{pauli} + \Delta E_{orb} \quad (6)$$

The first term refers to the electrostatic interaction energy between the fragments [26]. The prohibition to put two electrons with the same spin in a quantum cell generates the second term representing the repulsive interactions between the fragments (ΔE_{pauli}). The last term (ΔE_{orb}) designates the stabilizing orbital interaction contribution including the Heitler-London resonance phenomenon [27]. For noncovalent interaction, a general equivalent rising the gap between mathematical conception of the charge (and that of polarization) and physical reality is always blurred.

3-RESULTS AND DISCUSSION

3.1 GEOMETRICAL DETAILS

The complexes studied are labeled according to **Fig.1**. The relevant geometrical parameters are presented in **Table 1**. The majority of halide complexes have adopted preferentially the square planar configuration. Such a preferential square planar environment adopted has been confirmed experimentally by Yildirim et al [28]. Six notable exceptions (in which the plane containing the two halogen atoms and the TM (II) atom rotate around the M-N) have been revealed. This angle of rotation is variable: **4a** (31.4°), **5a** (19.2°), **5c** (29.4°), **3A** (36.7°), **4A** (40.1°) and **5A** (16.4°). Exceptionally for 3d TM chloride complexes, this configuration around the central metal is sensitive to multiplicity changes. This impact of multiplicity was highlighted by Minglian et al [29] during the study focused on the effects of structural modification on the ground state of metallabenzenes. This fact is attributed to the enhancement of electrostatic interaction. M-N and M-Cl bond distances within chloride nd^6 TM complexes are identical. The increase of the electronegativity of the counterion significantly induces those of the distances of the M-N bonds. The estimated average difference equal to 0.017Å is the result of the rise of the atomic radius. The solvation in the whole provokes a significant rise in the M-X bond distances with an average of the difference (in bond length) between the two media equal to 0.069 Å. The greater lability of M-X bonds in aqueous solution is thus disclosed. This lability more accentuated within the chloride complexes highlights the polarization effect of the counterion. This fact is in agreement with the drop of M...X interaction energy (in water) predicted by Canterford et al [30]. The inverse increase in M-X bond strength in the gas-phase complexes is consistent with Gaydon's [31] prediction arising from the analysis of microwave spectra of rotational features. Due to the lack of experimental data, the accuracy of our approach is only made by examining the FT-IR frequencies of the C=N stretching vibrational mode within 3d TM(II) complexes of (4-

methylbenzyl) aminoglyoxime ligand. Yildirim et al[28] reported that the frequency of this vibrational mode within the 3d TM complexes derived from glyoxime ligand falls in the range 1605-1610Hz. For B3LYP structures, the predicted frequencies are equal to 1647.9 and 1681.7 Hz for **3b** and **3c** respectively in gas phase. The N-M-N bond angles of chloride complexes involving TMs (II) of the same period are almost identical. For the 3d, 4d and 5d metal chloride series, the average is equal to 80.4, 77.4 and 78.1° respectively. But when the atomic number of the central metal rises along the period, the values of Cl-M-Cl bond angles become versatile. But, this fact provokes rather a drop in the Br-M-Br bond angle. For each bromide series, the highest values are observed for the nd^6 TM complexes.

Insert Figure 1

Insert Table 1

3.2. COMPLEX STABILITY

The total energy of each complex formed in various states (singlet (S) versus triplet (T) or doublet (D) versus quartet (Q)) is inserted in [Table 2](#). With the Exception of bromide iron (II) complexes, the negative energy difference between two spin states ($(\Delta E_{I-J}; I - J = S - T \text{ or } D - Q)$) of the majority of nd^6 TM complexes denotes the greater stability of higher multiplicity ones. Beyond 3d TM complexes, nd^7 and nd^8 TM complexes of both series prefer to adopt lower multiplicity state ([Fig 2 \(a\) and \(b\)](#)). Two plausible reasons can be determined: the strong overlap between the large xd orbitals ($x= 4$ and 5) and the ligand responsible for the drop in the pair energy of the electrons in these orbitals [32]. When atomic number of central TM rises, we detect an increase of ΔE_{I-J} values is detected in both cases. Overall, the thermodynamic parameters of complexation reported in [Table 2](#) are the energy, the enthalpy and the free energy complexation. Except for iron (II) complexes, nd^6 TM chloride complexes have the lowest are classified the following increasing order: **fourth period** < **fifth period** < **sixth period**. This trend remains the same for bromide complexes. [Table 2](#) also shows the increasing of complexation thermodynamic energies (enthalpy and free energy) with the increasing electronegativity of counterion in gas phase. For each identical TM, the average of the thermodynamic parameter difference reaches 421.3 and 416.9 kJ/mol respectively for complexation enthalpy and free energy values in this environment. All the negative values of these two thermodynamic parameters illustrate that the complexation process is exothermic and spontaneous in gas phase. Controversially, [Table 2](#) exhibits that the nature of this process depends on the type of halide complexes in water: this process

remains exothermic and spontaneous for chloride complexes. Meanwhile, contrary facts are obtained for bromide complexes. In the whole, the solvation of complexes analyzed conduct to the drastic drop of thermodynamic complexation parameters. For instance, the complexation enthalpies of chloride complexes are in the range 49-173 and 883-1011 kJ/mol in aqueous solution and gas phase respectively. This drastic reduction in complexation enthalpies due to the solvation process previously illustrated by Orzel et al [33] is due to the metal-counterion-solvent interaction. The negligible $T\Delta S^0$ values (Table 2) in comparison to the complexation enthalpies (ΔH^0) values exhibit the fact that these the complexation enthalpies are the dominant driving factors of complexation in solution.

Insert Table 2

Insert Figure 2

The additional descriptor of complex stability adopted is the metal ion affinity (MIA). Except for lower multiplicity complexes in the gas phase (Fig 3(a) and 4(b)), an augmentation of the MIA values is observed when the atomic radius of the divalent TM cation declines along a period: $na < nb < nc$ ($n = 3,5$ for X= Cl) and $nA < nB < nC$ ($n = 4,5$ for X= Br). For the single exception of palladium complex, we have recorded an augmentation of the MIA in the following order: $4b < 4a < 4c$ (chloride complex) and $4B < 4C < 4A$ (bromide complex). Overall, an agreement with the augmentation of MIAs reported by de Shanka et al [34] observed within cysteine complexes with metal cations (Li^+ , Na^+ , K^+ , Be^{2+} , Mg^{2+} and Ca^{2+}) is to be reported. But, this concordance is disrupted for the higher multiplicity complexes in each environment: for chloride complexes; $nb \approx nc < na$ ($n = 3,4$) and $5c < 5b < 5a$ and for bromide complexes; $nB < nC < nA$ ($n = 3,5$) and $4C < 4B < 4A$. This discordance (Fig 3(a), 4(b)) is more visible when moving from the fourth period to the sixth period in both nd^7 and nd^8 series: $4y < 3y \approx 5y$ (nd^7): $y = b, c$ (nd^8) (chloride complexes) $4B < 3B \approx 5B$ (nd^7): and $5C > 4C > 3C$ (nd^8) (bromide homologues). For higher multiplicity nd^6 metal complexes, we have rather the following sequence: $4a < 5a < 3a$ (chloride complexes) and $3A \approx 5A < 4A$ (bromide ones). Respectively for 3d and 4d TM chloride complexes at lower multiplicity, the solvation causes a very significant increase in MIA values with an average of 0.291 and 0.243 kcal/mol (Fig 4). The difference between the MIA values in aqueous solution and those in gas phase equal respectively on average to 0.309 and 0.243 kcal/mol is due to the steric repulsion effect ligand-ligand [35]. This repulsion effect is governed by the number of hydration molecules. The willingness to explore a possibility to correlate the retained charge on the central TM and the value of MIA is reflected in the

graphic junction of both parameters (Fig 1S). A proportional relationship between these two parameters is obtained for the chloride (nd^6 and nd^8) TM complexes except for 3d TM complexes (Fig 1S (a) and (b)): 3a and 3c. A similar trend is only observed for the nd^8 TM (bromide) complexes (Fig 1S (b)). On the contrary, an inverse proportionality is observed for nd^7 transition metals(bromide) complexes in gas phase. Similarly, the solvation of the complexes makes these two parameters inversely proportional for chloride (Fig 1S (c)) and bromide (Fig 1S (d)) nd^8 transition metal complexes. Within other aqueous complexes, a versatile correlation is observed.

The increase in the HOMO-LUMO gap in the lower multiplicity complexes (when the atomic number of the TM rises) is indicative of the drop in reactivity in the gas phase. (Fig 5 (a)). The majority of 3d TM complexes show more reactivity in this medium. The solvation of these 3d TM complexes (with the exception of the cobalt complexes in both series) has been shown to alter their reactivity (Fig 5 (b)). Due to this solvation, the HOMO-LUMO gap drops on average by 31 kJ/mol. This disturbance of the reactivity by solvation is found to be more emphasized within the bromide complexes. Overall, larger HOMO-LUMO gap values have been observed for the lower multiplicity molecular systems. The average difference in calculated HOMO-LUMO deviations is around 63.8 and 61.4 kJ/mol for the chloride and bromide complexes, respectively. This suggests that the electrostatic attraction is more pronounced in the lower spin state.

Insert Figure 3

Insert Figure 4

Insert Figure 5

3.3. BONDING PROPERTIES

The topological parameters of M...N interactions within optimized complexes (instantaneous interatomic interaction energy, electron density, laplacian of electron density, kinetic energy density $G(r)$, potential energy density $V(r)$, total energy of electron ($H(r)$ and ellipticity of the metal-ligand bond (ϵ)) are presented in Table 3. A second derivative at critical points (BCP)) of the electron density calculated in terms of values of the Laplacian is positive in both media. The electron densities of the M-N bond are found to be lower within the higher multiplicity chloride complexes (gas phase (Fig 2S (a)) and water (Fig. 2S (b))). This fact is evidence that the weakest bonding strength in this higher multiplicity state. The great importance of the M-N interatomic interaction within the higher multiplicity chloride complexes agrees with the

geometrical reality (Table 1 and 3). This fact is evidence that this higher multiplicity corresponds to the lowest bonding strength. Similar observations have been found within the bromide complexes. Collectively, the M-N electron density values are less than 0.1 a.u. The gradient values range from 0.2356 to 0.6962 (a.u) in vacuum and from 0.2583 to 0.7219 (a.u) in water (Table 3). From these positive values, we can conclude that the electron density is concentrated towards the basin around each atomic partner of the said interaction. Therefore, the net repulsion forces is acting on the involved nuclei (N and M). The average ratio ($-G(r)/V(r)$) equal to 0.7667(vacuum) and 0.8435(water) is comprised between 0.5 and 1 for the M...N interactions within the chloride complexes. For bromide complexes, the averages of these ratios are respectively equal to 0.8560 and 0.8880. In the whole, the three above-mentioned constraints ($\rho(r) < 0.1a.u$, $\nabla^2\rho(r) > 0$ and $0.5 < -G(r)/V(r) < 1$) are confirming the intermediate partially covalent nature of the M-N bond. Regardless of the counterion adopted, the exceptional rise (in both study environments) of this ratio beyond 1 for the both series reveals the pure non-covalent nature of the M... N bond for Co^{2+} and Ni^{2+} complexes at higher multiplicity. In both study media, the geometrical optimizations are dominated by H...X interaction (X = Cl, Br) with the exception of the Fe^{2+} bromide complex (**3A**) in which this interaction is completely null (in vacuum). The different X...H binding energies (Fig 6 (a, b, c and d)) ranging from 3 to 10 kcal/mol prove that these interactions are vander Waal type. Three factors influencing the sensitivity of the bonding strength have been found: (i) the nature of the halogenated ligand (ii) the spin multiplicity, (iii) the study medium. The H...X bonding strength have shown to be most pronounced for higher multiplicity complexes in aqueous solution (Fig 6 (b) and (d)) with three specific exceptions of chloride complexes (Fe^{2+} (**3a**), Ir^{2+} (**5b**) and Pt^{2+} (**5c**) complexes: (Fig 6 (b)). Overall, the negative λ_1 and λ_2 eigenvalues of the Hessian matrix at the critical point of the M-X bonds (Table 1S: X=Cl and Br) is a sign that the curvature of the electron density is perpendicular to the M-X bond in the both study media. Consequently, the local concentration of the electronic charge within the interatomic region is covalent or polarized. For comparative measurement of the stability of bonds, the ellipticity has been adopted as a descriptor. The highest value of ellipticity agrees with the most unstable bond [36]. The metal-halogen bonds within the lower multiplicity complexes are found to be the most unstable compared to their metal-nitrogen counterpart in both media (Fig 7 (a), (b), (c) and (d)). This greater lability of the former is due to the high electronegativity of halogen atoms. For both counterion series, the instability of

metal-nitrogen bonds within the higher multiplicity nd^7 TM complexes is more accentuated in vacuum (Fig 7 (a) and (b)). The metal-halogen bonds of higher multiplicity complexes remain the most unstable in aqueous solution. Some exceptions of bromide complexes (3C, 4B and 5B) are worth mentioning (Fig 7 (c), and (d)). In addition, The TM-nitrogen bonds within nd^7 and nd^8 (higher multiplicity) TM complexes of both series are more unstable in both media.

Table 3

Insert Figure 6

Insert Figure 7

The comparative analysis of the Wiberg indices of these two bonds displays the superiority of the bond strength of the TM-halogen bonds in the two media studied (Table 2S and Fig 8(a) and (b)). Regardless of the medium, the passage from the chloride complex to the bromide one of the same TM causes a non-significant alteration in the M-N bonding strength: the average of the differences between the Wiberg index of the chloride complex and that of the bromide one of the same TM is equal to 0.01758 and 0.003178 in gas phase and in water, respectively, for the chemical library. The OH...X (X=Cl and Br) interactions in the bromide complexes are found to be slightly stronger than their chloride counterparts (Table 2S and Fig 8 (c)). In both media, this interaction is exceptionally stronger within the fourth period TM chloride complexes. This reinforcement of this interaction is observed when the atomic number of the TM increases along the period. For the Ruthenium complex, the huge gap (0.0568: Table 2S and Fig 8 (c)) in Wiberg index between the chloride and bromide structures expresses the remarkable strengthening of the OH... X interaction. The higher Wiberg index values of the low-multiplicity structures further confirm the higher bonding strength of the M-N and M-X bonds (Table 2 and (Fig 8(d))). In order to obtain a more explanation of the $M^{2+} \rightarrow N$ interaction, we have proceeded by energy decomposition of the total [glyoxime ligand] \rightarrow $[MX_2]$ interaction energy by means of an adaptive EDA(Fig 9). The minor contribution the energy required (ΔE_{prep}) to promote the two fragments in the estimates has been neglected in this analysis The different contributions of this total interaction energy are reported in the Table 4.

Insert Figure 8

Insert Figure 9

Except for chloride iron complex (3a), the differences between the interaction energies of lower multiplicity complexes and those of higher multiplicity ones with the same counterion

are found to be negative (Fig 10 (a) and (b)). Therefore, the stronger interaction within the lower multiplicity complexes explains our exclusive limitation to them in the further analysis of this decomposition. For ΔE_{int} values of TM complexes of the same period, an enhancement of the [glyoxime ligand] \rightarrow $[MX_2]$ interaction strength is noticed in the following order (Fig 11: (a), (b), (c) and (d)): $Fe^{2+} < Co^{2+} < Ni^{2+}$ (3d), $Pd^{2+} < Rh^{2+} < Ru^{2+}$ (4d) and $Pt^{2+} < Ir^{2+} < Os^{2+}$ (5d). Regardless of the environment, these interaction forces augment within a column of the periodic table for a selection of central TM carried from top to bottom in both series. Overall, the observed negative electrostatic contribution (ΔE_{els}) reflects the overcoming of the singular nuclear repulsion. This overcoming causes an interpenetration effect of charge clouds at a very short distance [glyoxime ligand] \rightarrow $[MX_2]$ [37]. The lower multiplicity complexes in both series exhibit [glyoxime ligand] \rightarrow $[MX_2]$ interactions that are more electrostatic than orbital regardless of the media studied (Table 4). In the gas phase, the electrostatic contribution (ΔE_{els}) ranges from 51.4-99.4 % and 45.2-99.2% for chloride and bromide complexes respectively. These ranges become respectively equal to 51.7- 99.4 % and 45.7-96.4 % in aqueous solution. The electrostatic interaction strength appears to be higher for the chloride nd^7 and nd^8 TM complexes (Table 4). Therefore, the poor coordination of the bromide ligand to the central TM reported by Jaga [38] is confirmed. An exceptional closeness between the two (electrostatic and orbital) interaction forces within the nd^6 TM complexes has been detected. Except for the palladium complexes (4x: x = c and C), this closeness of the two forces is extended within all the complexes examined by solvation.

Table 4

Insert Figure 10

Insert Figure 11

In general, the orbital contributions are very minor. For exceptional cases found, the maximal orbital contributions match up with the osmium complexes of the series : **5a** (-856.9 kJ/mol) **5A** (-1088.2 kJ/mol) in gas phase and **5a** (-878.7 kJ/mol) and **5A** (-1106.5 kJ/mol) in water. Our results demonstrate that these maximal orbital contributions are correlated to maximal dissociation and interaction energies. In both environments, the prudence to make a generalisation of this fact, emitted by Frenking et al [39], remains valid for all the complexes of the two series: For the 3d transition metals chloride complexes in the gas phase, the maximal orbital contribution (3a: -19.8kJ/mol) corresponds instead to a minimal parameters (dissociation energy (361 kJ/mol) and interaction energy (-359.5kJ/mol) (Fig 11(a)). Similarly,

for chloride 4d TM complexes in water, the palladium complex with its maximal orbital contribution (-92.9821 kJ/mol) displays instead a minimal dissociation (444 kJ/mol) and interaction(-442.728kJ/mol) energy values (Fig 11(c)). The break of correlation may be due to the simultaneous involvement of electrostatic attraction and Pauli repulsion compensating the small difference in ΔE_{orb} [40].

4-CONCLUSION

In the present paper, we have studied the $[MLX_2]$ complexes resulting from chelation of nd^x ($x = 6,7$ and 8) transition metal(M) to glyoxime ligand (L) and to two halogen ligands ($X = Cl$ and Br). A tailoring basis combined to B3LYP functional: nd^x ($x= 6,7$ and 8) transition metals and halogen atoms (Br and Cl) has been used while other atoms are described using polarized and diffuse triple Pople basis set (6-311++G(d,p)). The square planar configuration has been preferred by the lower multiplicity optimized structures in their majority. Highest X-M-X bond angles have obtained for nd^6 bromide complexes traducing the highest repulsion between the two bromide atoms. The multiplicity changes lead to the alteration of this coordination sphere with exception for 3d chloride complexes. Such an alteration is due to the enhancement of electrostatic interaction. The sensitive augmentation of the M-X bond distances induced by solvation highlighting its higher lability in aqueous solution may be the polarization effect of halide ligands. The energy complexation of the complexes in both series can be classified according the period of the TM: fourth period < fifth period< sixth period. For majority of lower multiplicity complexes in gas phase, an augmentation of the MIA values when the atomic radius of the divalent TM cation declines along a period: $na < nb < nc$ ($n =3,5$ for $X= Cl$) and $nA < nB < nC$ ($n =4,5$ for $X= Br$). The solvation of the complexes makes the retained charge on the central metal is inversely proportional to the values of MIA for both nd^8 TM complexes. In the basis of the ellipticity as a descriptor, the TM-halogen bonds within the lower multiplicity complexes have shown to be the most unstable than their metal-nitrogen counterpart in both media. The Energy decomposition of Morokuma indicates that the [glyoxime ligand] \rightarrow $[MX_2]$ interaction strength is growing in the following order $Fe^{2+} < Co^{2+} < Ni^{2+}$ (3d), $Pd^{2+} < Rh^{2+} < Ru^{2+}$ (4d) and $Pt^{2+} < Ir^{2+} < Os^{2+}$ (5d). It also demonstrates that that these interaction strengths in a column of the periodic table tends to increase from the top to the bottom in both series regardless of the environment.

COMPLIANCE WITH ETHICAL STANDARDS

Conflict of interest. The authors declare that they have no conflict of interest.

ACKNOWLEDGEMENT

This work was supported by the Ministry of Higher Education of Cameroon.

REFERENCES

1. Thomas TW and Underhill AE (1972). *Chem Soc Rev*: vol. 1, p. 99.
2. İrez G, and Bekaroğlu Ö(1983). *Synth React Inorg Met -Org Chem* 13: 781.
3. Serin S, and Bekaroğlu Ö, *Anorg Z*(1983). *Allg Chem*, vol 496 (197):197.
4. Gök Y, and Serin S.(1988). *Synth. React. Inorg Met. -Org Chem* 18 :975.
5. Asghari SM, Khajeh K, Moradian F, Ranjbar B and Naderi-Manesh H(2004). Acid-induced conformation changes in *Bacillus* 39:51-57.
6. Alanis AJ(2005). *Archives of Medical Research* 36(6): 697-705.
7. Schrauzer GN, Windgassen RJ and Kohnle J(1965). *Chem Ber* 98:3324.
8. Brown BG(1973) *Prog. Inorg. Chem* 18: 17.
9. Underhill AE, Watkins DM and Petring R(1973). *Inorg Nucl Chem Lett.*9: 1269-1273.
10. Chakrovorty A (1974). *Rev Coord Chem* 13:1-46.
11. Deveci P, Taner B, Kılıc Z, Solak A.O, Arslan U, Özcan E (2011). *Polyhedron* 30 : 1726–1731.
12. Durmus M, Ahsen V, Luneau D, Pecaut J (2004). *Inorg Chimica Acta* vol. 357, no. 2,p. 588.
13. Hayati S, Muzaffer C and Mustafa M (2005). *Acta Chimica Slovenica*, 52: 317-322.
14. Ulku S, Omer D, Ercan T, and Ayhan O(2012), 81: 146-151.
15. L.N. Nogheu, J.N. Ghogomu, D.B.Mama, N.K. Nkungli, E. Younang, and S.R. Gadre, *Computational Chemistry*,4, (2016),119-136.
16. M. Kurtoglu, E. Ispir, N. Kurtoglu and S. Serin, “Novel vic-dioximes: Dyes Pigments, 77, (2008), 75-80.
17. R. B. Singh, B. S. Garg and R. P. Singh, *Oximes as Spectrophotometric Reagents-a Review Talanta* Vol. 26, (1979),PP. 425-444.
18. Arash ALIZADEH YEGANI1, Gülüzar ÖZBOLAT2, Abdullah TULI2, Removal of heavy metals from wastewater by using dimethylglyoxime ligand. *ACTA BIOLOGICA TURCICA* 30(1): 22-26, 2018
19. Frisch MJ, Trucks GW, Schlegel HB, Scuseria GE, Robb MA, Cheeseman JR, Montgomery JA, Vreven T, Kudin KN, Burant JC, Millam JM, Iyengar SS, Tomasi JJ, Barone V, Mennucci B, Cossi M, Scalmani G, Rega N, Petersson GA, Nakatsuji H, Hada M, Ehara M, Toyota K, Fukuda R, Hasegawa J, Ishida M, Nakajima T, Honda Y, Kitao O, Nakai H, Klene M, Li X, Knox JE, Hratchian HP, Cross JB, Adamo C, Jaramillo J, Gomperts R, Stratmann RE, Yazyev O, Austin AJ, Cammi R, Pomelli C, Ochterski JW, Ayala PY, Morokuma K, Voth A., Salvador P, Dannenberg JJ, Zakrzewski VG, Dapprich S, Daniels AD, Strain MC, Farkas O, Malick DK, Rabuck AD, Raghavachari K, Foresman JB, Ortiz JV, Cui Q, Baboul AG, Clifford S, Cioslowski J, Stefanov BB, Liu G, Liashenko A, Piskorz P, Komaromi I, Martin RL, Fox DJ, Keith T, Al-Laham MA, Peng CY, Nanayakkara A, Challacombe M, Gill PMW, Johnson B, Chen W, Wong MW, Gonzalez C, Pople JA, (2009). *Gaussian 09 Revision B.04* Gaussian Inc Pittsburgh: PA (Licence G09).
20. Grimme S, Antony J, Ehrlich S, Krieg AH (2010) .Consistent and accurate ab initio Parametrization of Functional Dispersion correction (DFF-D) for 94 elements H-Pu, J

Chem Phys 132 :154104-154119. Ivanciuc O, Balaban AT (1998) Graph theory in chemistry. In: PVR S, Allinger NL, Kollmann PA, Clark T, HFS S, Gasteiger J, Schreiner PR (eds) The encyclopedia of computational chemistry. John Wiley & Sons, Chichester 1169–1190

21. Marino T, Russo N, Toscano M (2000). Gas-phase metal ion (Li^+ , Na^+ , Cu^+) affinities of glycine and alanine, *J Inorg Biochem* 79 :179-185
22. Lu T, Chen F (2012) . Multiwfn: a multifunctional wavefunction analyzer, *J Comp Chem* 80: 335 -592.
23. Reed AE, Curtiss LA, Weinhold F (1988) . Intermolecular interactions from a natural bond orbital, donor-acceptor viewpoint, *Chem. Rev.* 88 :899-926.
24. K. Morokuma, Molecular orbital studies of hydrogen bonds (1971). III. $\text{C}=\text{O}\dots\text{H}-\text{O}$ hydrogen bond in $\text{H}_2\text{CO}\dots\text{H}_2\text{O}$ and $\text{H}_2\text{CO}\dots 2\text{H}_2\text{O}$, *J Chem. Phys.* 551 :236-1244.
25. Ziegler T, Rauk A, Baerend EJ (1976). The electronic structures of tetrahedral oxo complexes. The nature of the charge transfer, *Chem Phys* 16 : 209-217.
26. Wysokinski R, Michalska D (2001). The performance of different density functional methods in the calculation of molecular structures and vibrational spectra of platinum (II) antitumor drugs: cisplatin and carboplatin, *J Computer Chem* 22 : 901-912.
27. Pauling LC (1960). *The Nature of the Chemical Bond*, third ed, Cornell University Press, Ithaca, NY.
28. Yildirim B, Özcan E, Deveci P (2007). *Russian Journal of Coordination Chemistry*, Vol. 10, (6): 417–421.
29. Minglian L, Pengfeli L and Zexing C (2011). *Journal of theoretical and computational chemistry* Vol. 33, (6): 861-874.
30. Centerford JH, Calton (1968). *Halides of 2nd and 3rd row transition metals* wiley Interscience.
31. G. Gaydon (1968). *“Dissociation Energies and Spectra of Diatomic Molecules,”* 3rd ed., Chapman and Hall, London.
32. Stephens PJ, Devlin FJ, Chabalowski CF, Frisch MJ (1994). *Journal of Physical Chemistry*, Vol. 98, (45): 11623-11627.
33. Orzeł Ł, Was J, Kania A, Susz A, Rutkowska-Zbik D, Staron J, Witko M, Stochel G, Fiedor L (2017). Factors controlling the reactivity of divalent metal ions towards pheophytin a. *J. Biol Inorg. Chem.* 941–952.
34. Shankar R, Kolandaivel P, Senthilkumar L (2011). Interaction studies of cysteine with Li^+ , Na^+ , K^+ , Be^{2+} , Mg^{2+} and Ca^{2+} metal cation complexes, *J Phys Org Chem* 24 :553-567.
35. Ingmar Persson (2010). Hydrated metal ions in aqueous solution: How regular are their structures? *Pure Appl. Chem.*, Vol. 82, (10): 1901–1917.
36. Nozad AG, Meftah S, Ghasemi MH, Kiyani RA, Aghazadeh M. (2009), *Biophys Chem* 141: 49.
37. Bickelhaupt FM, Baerends EJ, Kohn-Sham (2000). density functional theory: predicting and understanding chemistry, *Rev. Comp. Chem.* 15: 1-86.
38. Jagadeesan R, Velmurugan G, Venuvanalingam P (2015). *RSC Adv* 5 : 80661–80667.

39. Frenking G, Miquel Sola, Sergei F. Vyboishchikov (2005). Chemical bonding in transition metal carbene complexes, *Journal of Organometallic Chemistry* 690 :6178–6204
40. Frenking G, Wichmann K, Fröhlich N, Grobe J, Golla W, Le Van D, Krebs B, Lage M(2002):A case where the trend of the overall bond strength becomes determined by the electrostatic term has recently been reported for phosphane complexes, *Organometallics* 21 (CO)5TM–PR3. 2921.

Figures

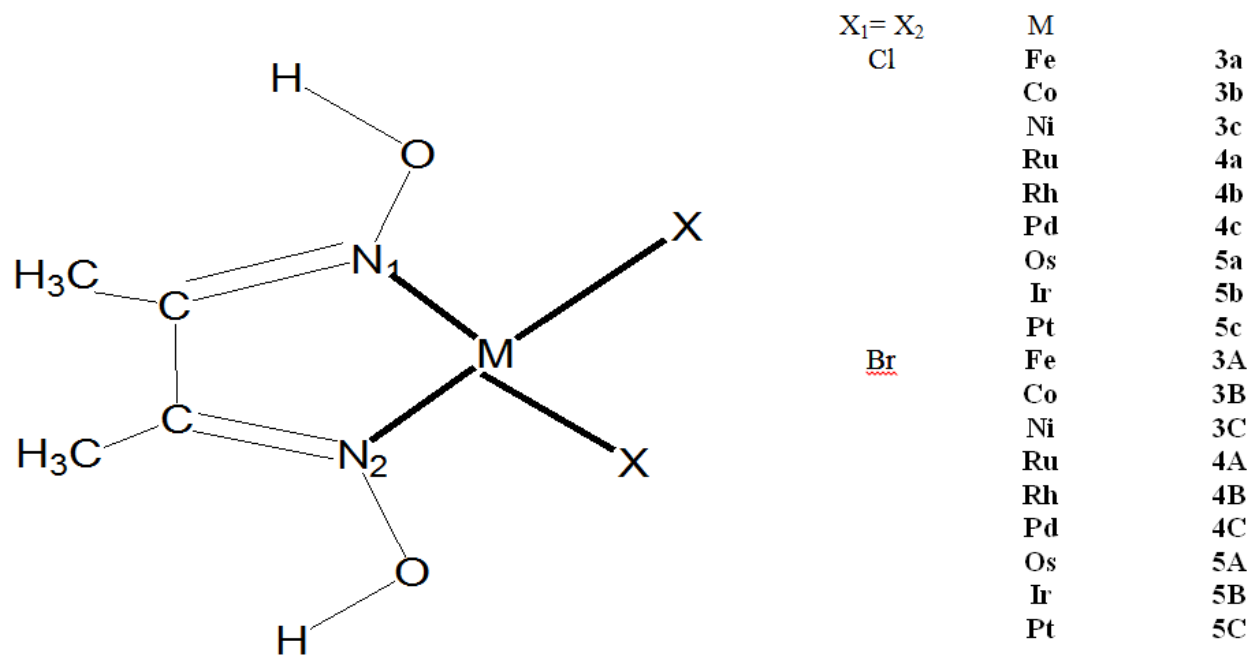


Figure 1: Molecular library and numbering systems adopted for complexes analyzed

Figure 1

Figure 1: Molecular library and numbering systems adopted for complexes analyzed

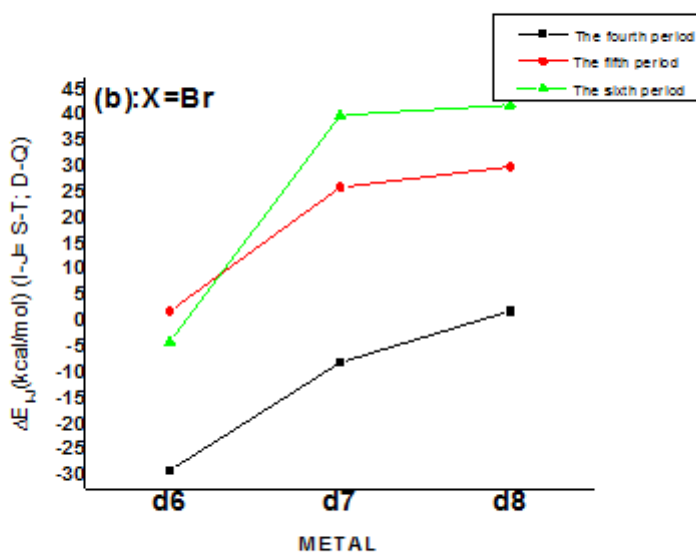
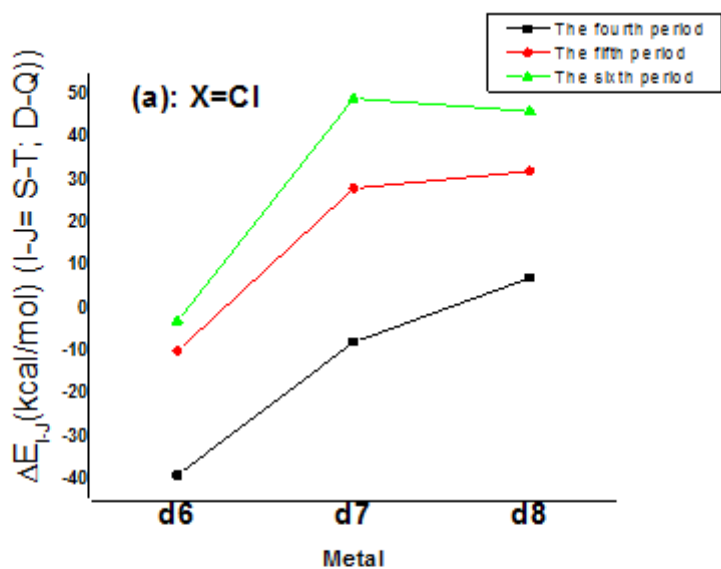


Figure 2: Predicted ΔE_{I-J} (I-J=S-T, D-Q) values of nd^x (n = 3-5; x = 6-8) chloride ((a) bromide (b) complexes.

Figure 2

Figure 2: Predicted ΔE_{I-J} (I-J=S-T, D-Q) values of nd^x (n = 3-5; x = 6-8) chloride ((a) bromide (b) complexes.

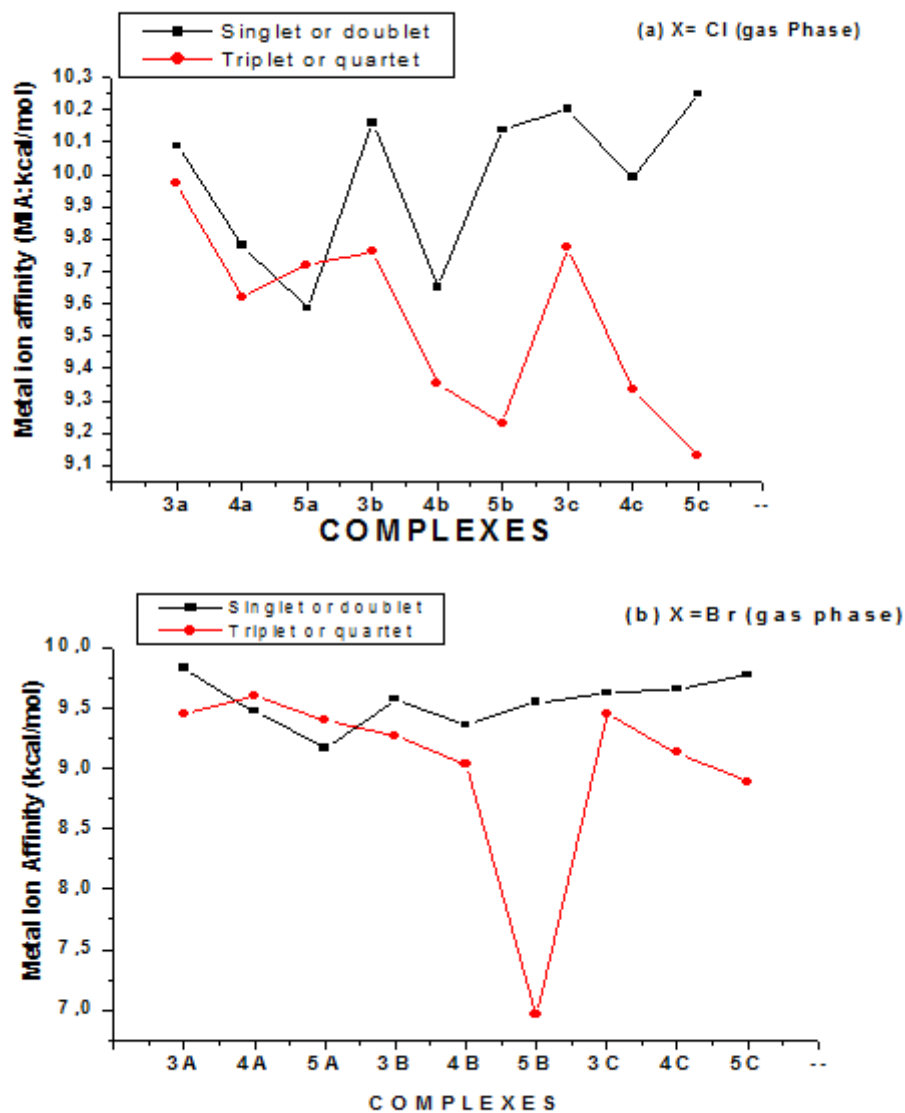


Figure 3. Comparative influence of multiplicity on metal ion affinity in chloride (a) and bromide (b) at B3LYP/Gen level in gas phase.

Figure 3

Figure 3 : Comparative influence of multiplicity on metal ion affinity for chloride (a) and bromide (b) complexes at B3LYP/Gen level in gas phase.

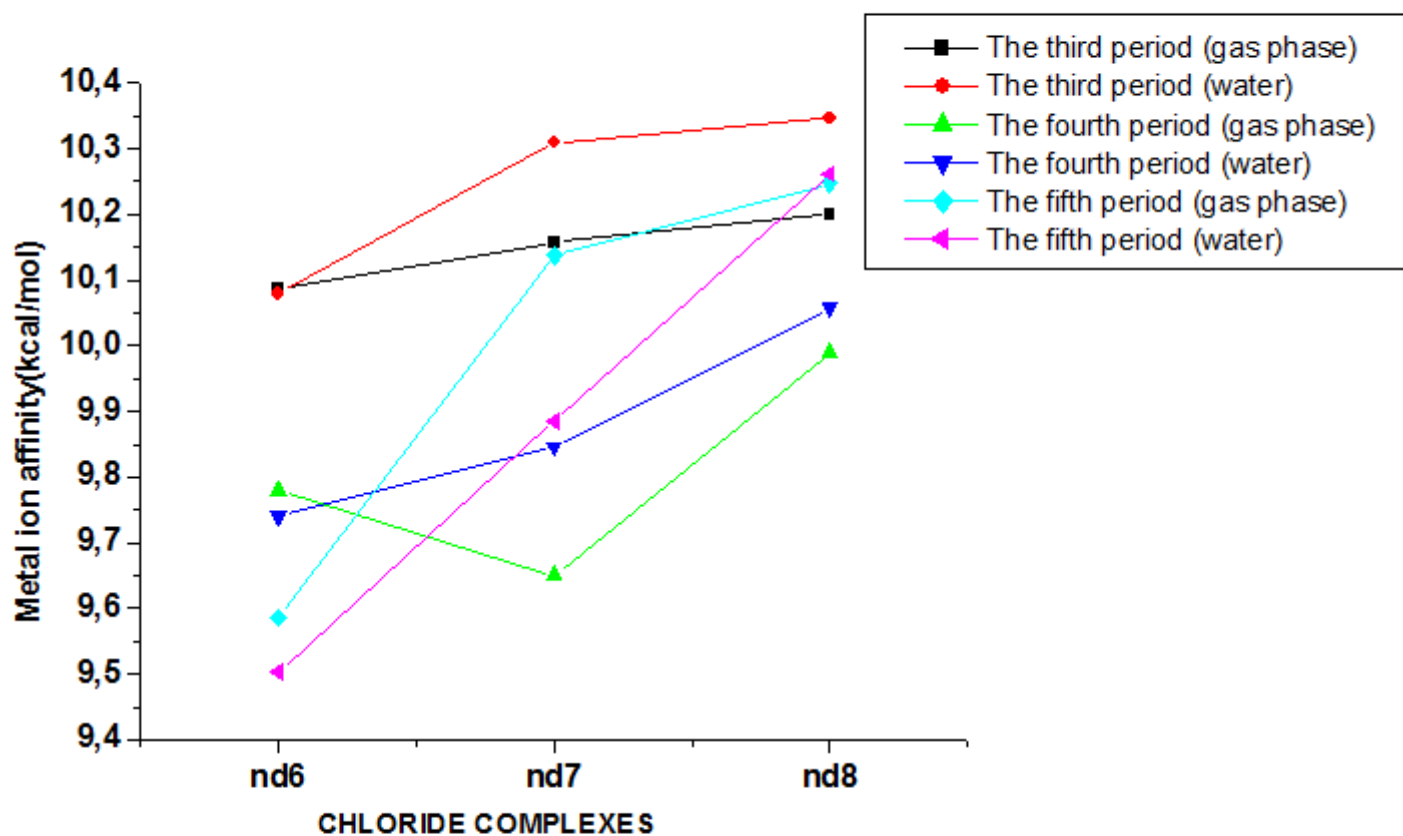


Figure 4 : Comparative influence of multiplicity on metal ion affinity at B3LYP/Gen level in both study media for chloride complexes.

Figure 4

Figure 4 : Comparative influence of multiplicity on metal ion affinity at B3LYP/Gen level for chloride complexes in both study media

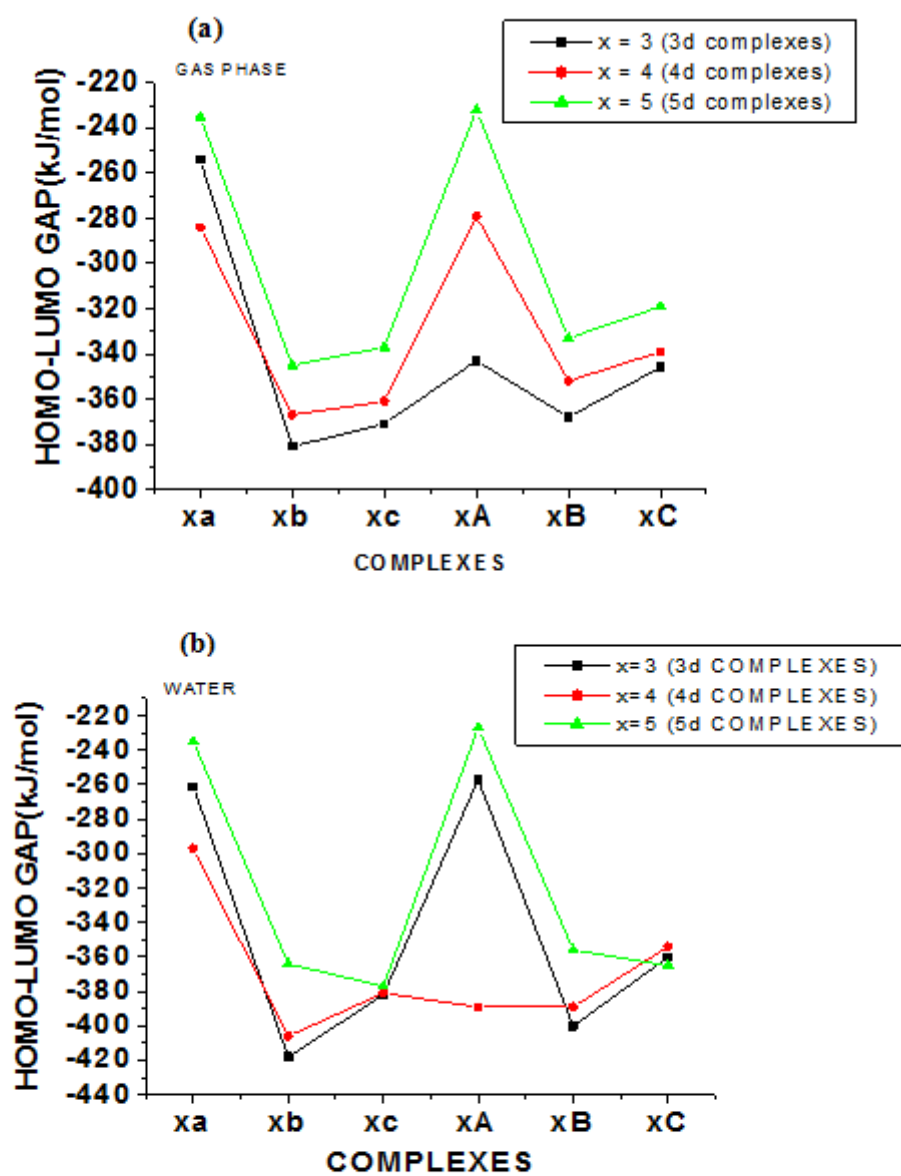


Figure 5: HOMO-LUMO gap (in kJ/mol) of nd^x ($n = 3-5$; $x = 6-8$) halide complexes in gas phase (a) and water (b).

Figure 5

Figure 5: HOMO-LUMO gap (in kJ/mol) of nd^x ($n = 3-5$; $x = 6-8$) halide complexes in gas phase (a) and water (b).

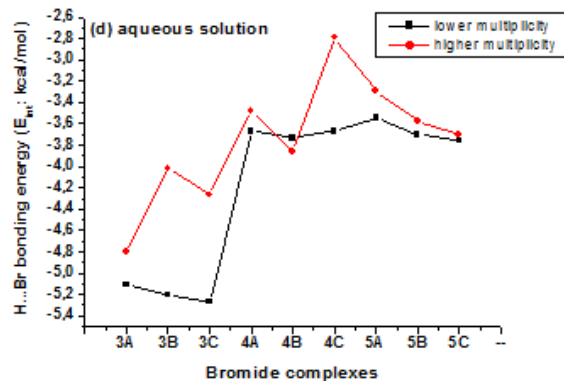
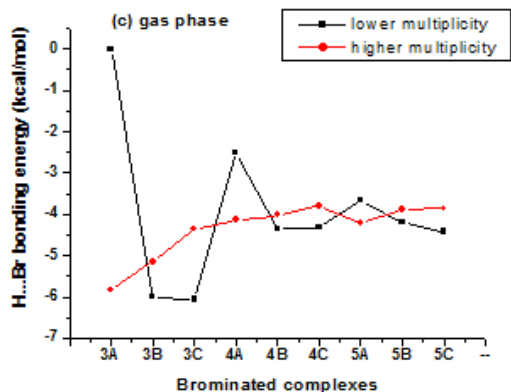
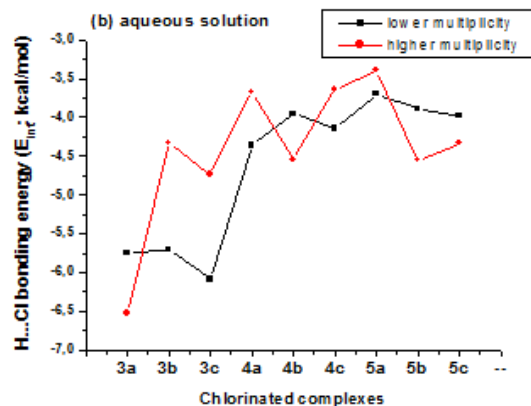
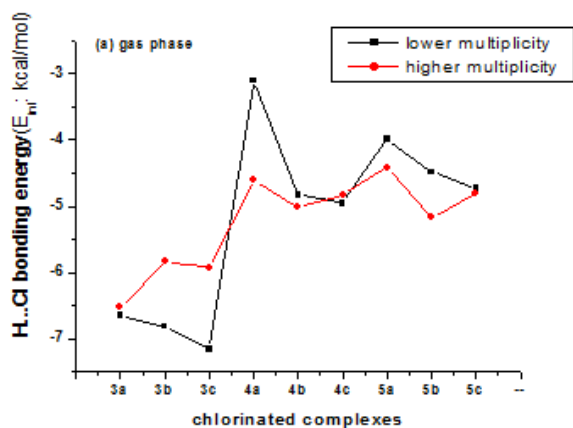


Figure 6: X ...H (X= Cl (a,b) or Br (c,d)) bonding energies within optimized complexes at B3LYP/GEN

Figure 6

Figure 6: X ...H (X= Cl (a,b) or Br (c,d)) bonding energies within optimized complexes at B3LYP/GEN

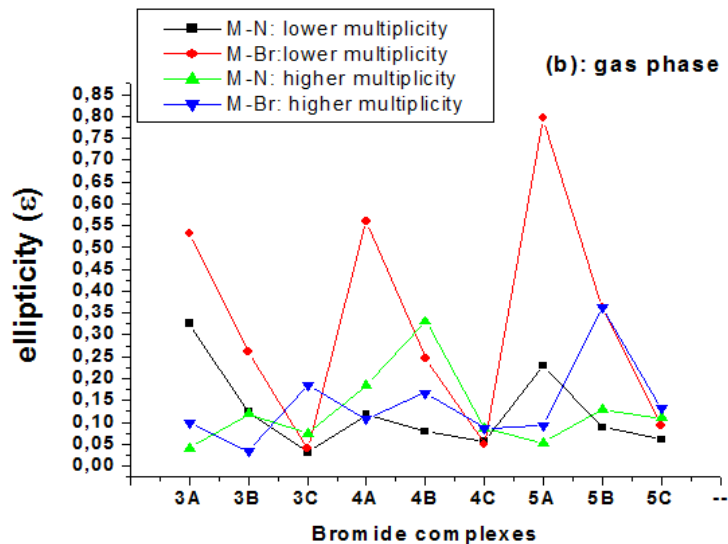
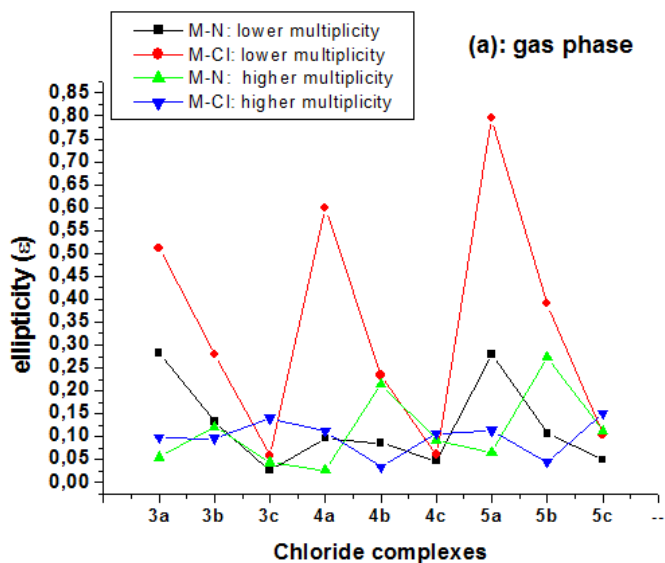


Figure 7

Figure 7: ellipticity of chloride and bromide transition metal complexes at various multiplicities.

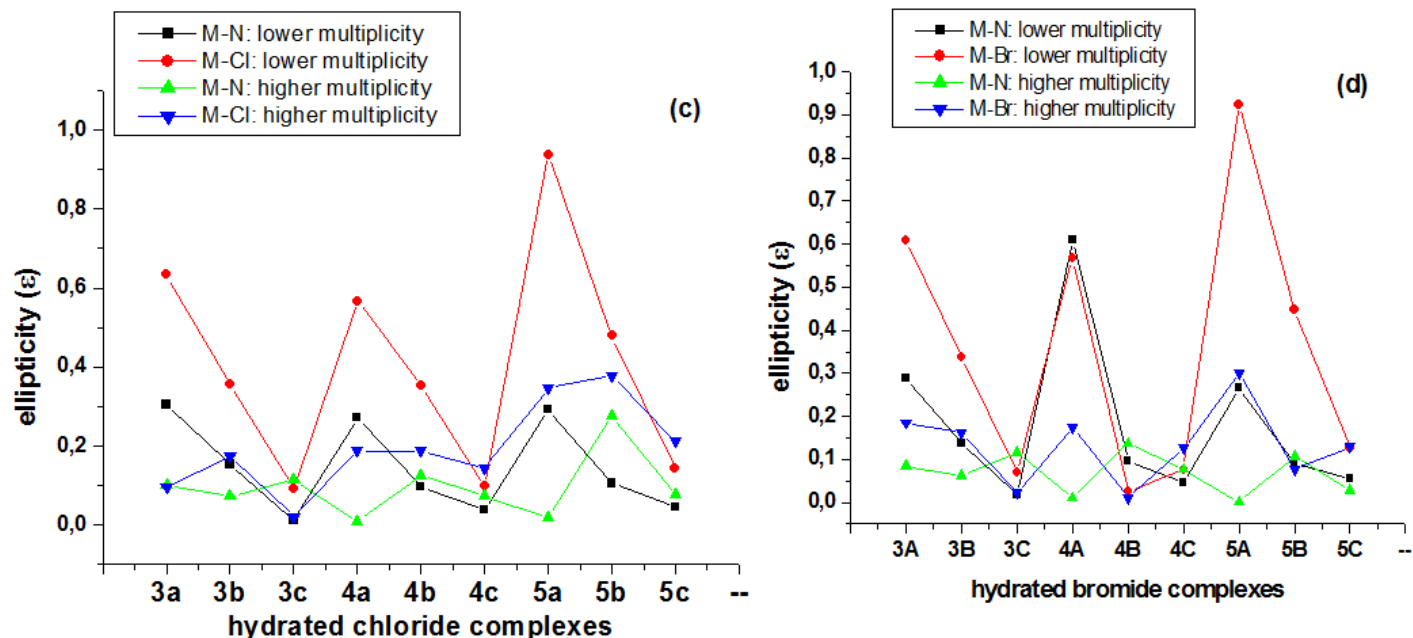


Figure 7: ellipticity of chloride and bromide transition metal complexes at various multiplicities.

Figure 8

Figure 8: M...N, M...X and O-H...X (X= Cl and Br) Wiberg bond indexes of halide complexes in various media.

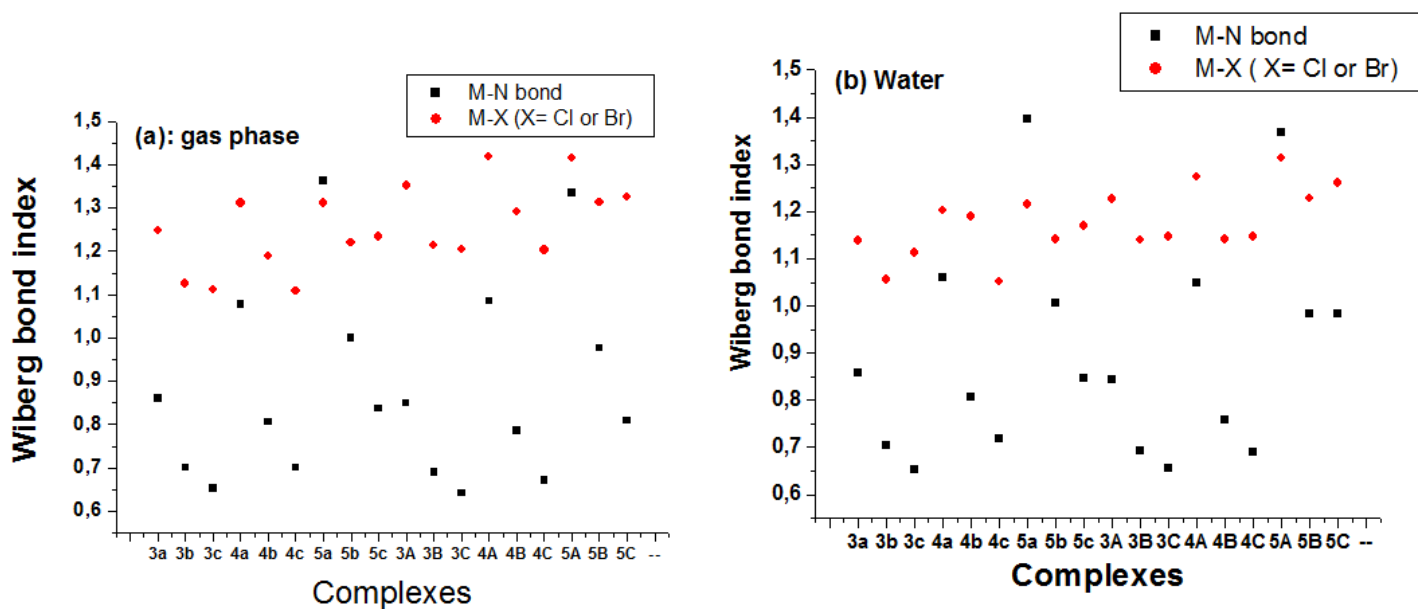


Figure 9

Figure 8: Graphical illustration of fragments considered for EDA to explore [glyoxime ligand] [MX₂] interaction within complexes.

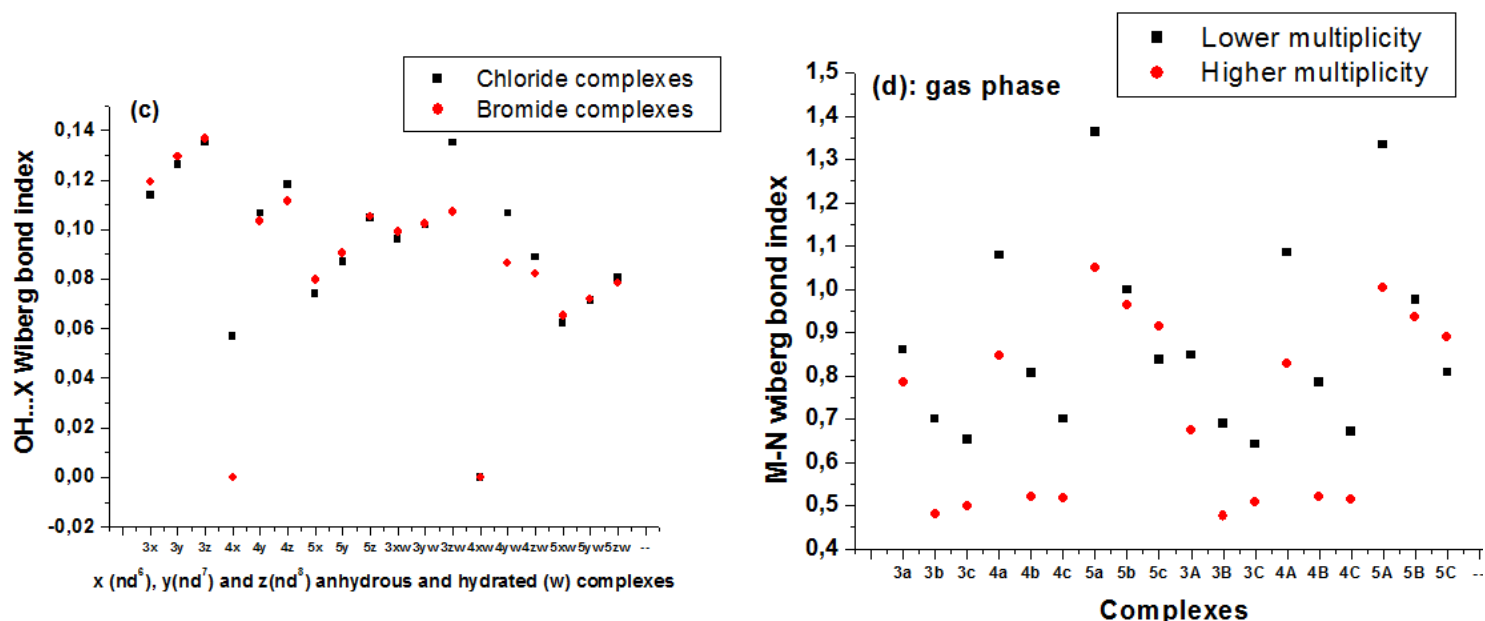
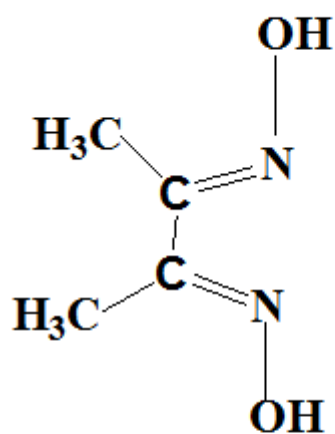


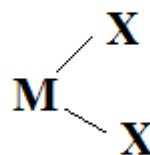
Figure 8: M...N, M...X and O-H...X (X= Cl and Br) Wiberg bond indexes of halide complexes in various media.

Figure 10

Figure 8: Graphical illustration of fragments considered for EDA to explore [glyoxime ligand] [MX₂] interaction within complexes.



Fragment 1: glyoxime ligand



Fragment 2: [MX₂]

Figure 9: Graphical illustration of fragments considered for EDA and CDA to explore [glyoxime ligand] [MX₂] interaction within complexes.

Figure 11

Figure 9: Graphical illustration of fragments considered for EDA to explore [glyoxime ligand] ... [MX₂] interaction within complexes.

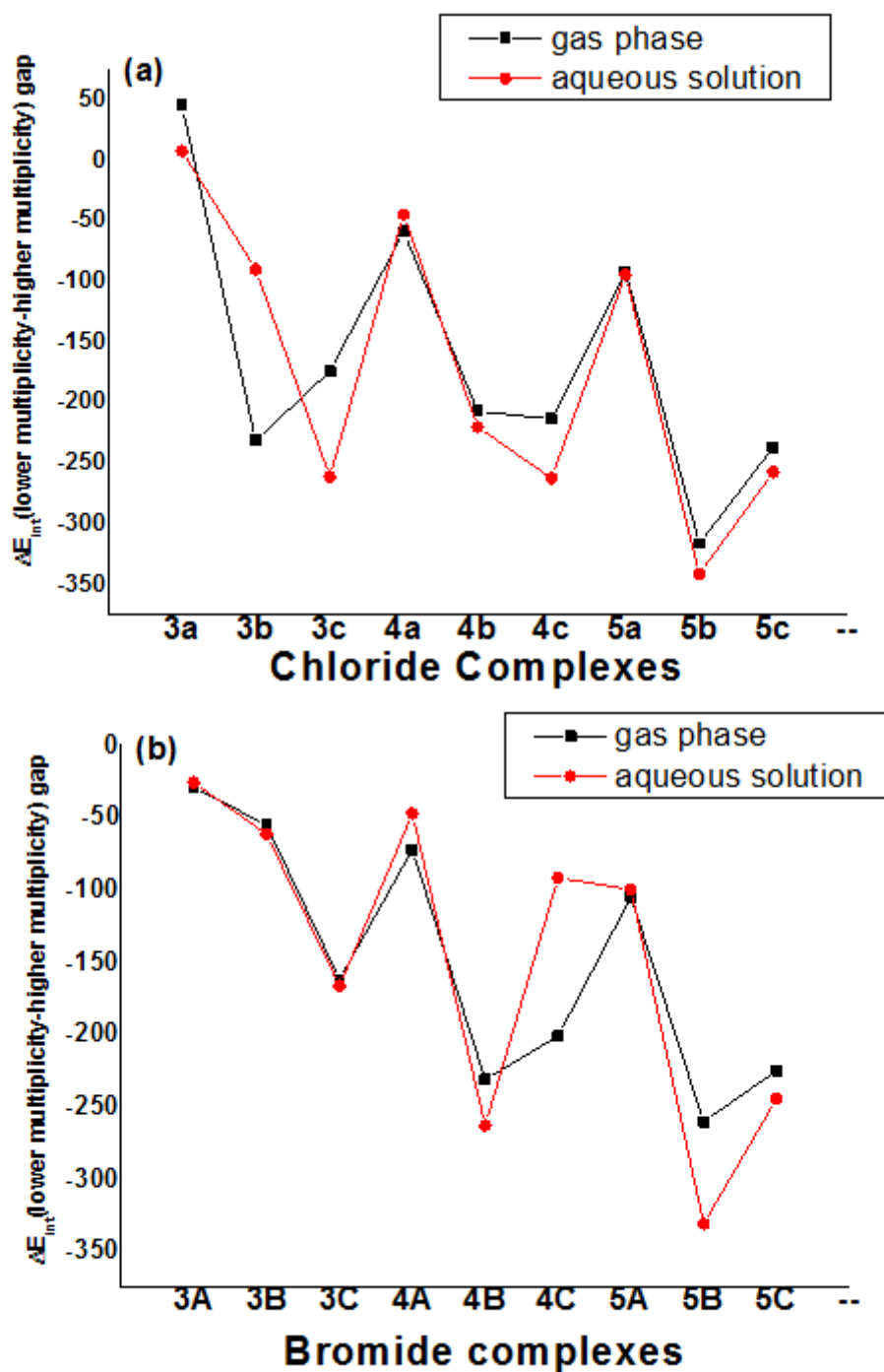


Figure 10: Interaction energies (ΔE_{int}) of the complexes of the two series in lower multiplicity (or in higher multiplicity) in the study environment.

Figure 12

Figure 10: Interaction energies () of the complexes of the two series in lower multiplicity (or in higher multiplicity) in the study environment.

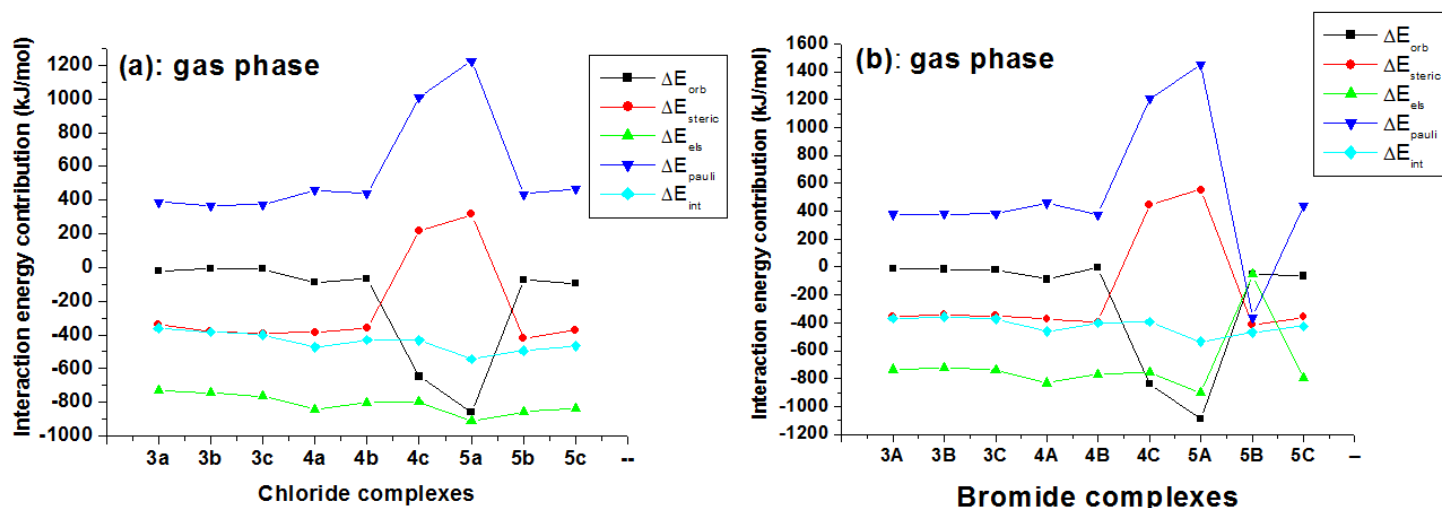


Figure 13

Figure 11: Graphical comparative interaction energy contribution of chloride (a and c) and bromide (b and d) complexes in gas phase (a and b) and in water (c and d).

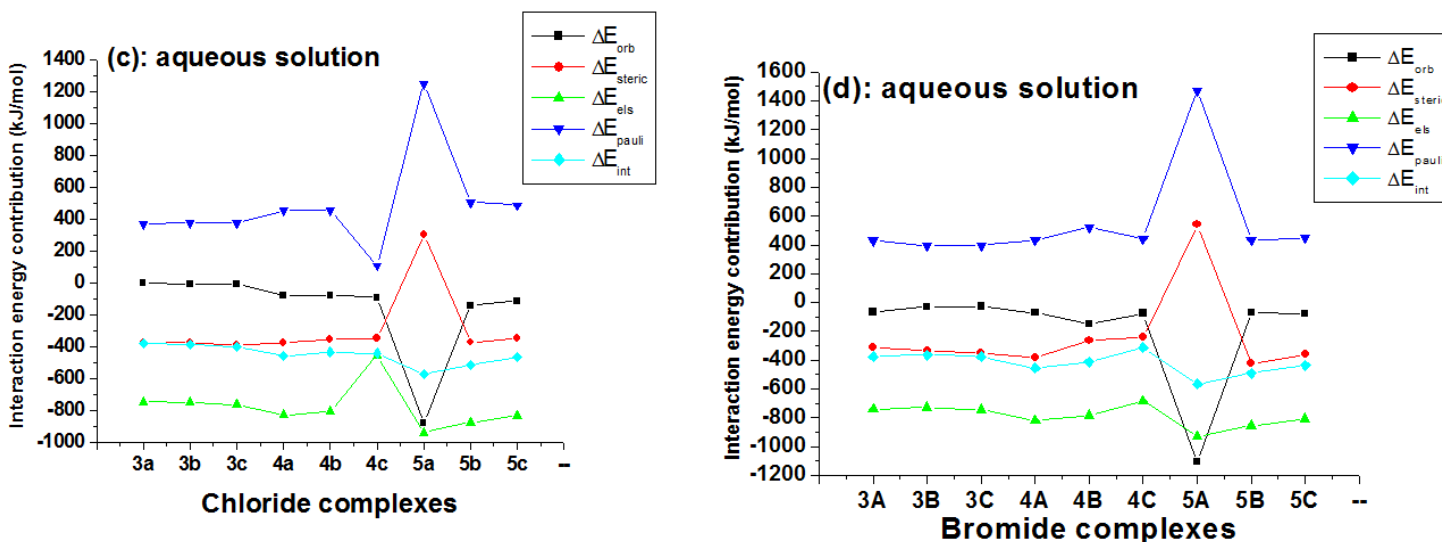


Figure 11: Graphical comparative interaction energy contribution of chloride (a and c) and bromide (b and d) complexes in gas phase (a and b) and in water (c and d).

Figure 14

Figure 11: Graphical comparative interaction energy contribution of chloride (a and c) and bromide (b and d) complexes in gas phase (a and b) and in water (c and d).

Supplementary Files

This is a list of supplementary files associated with this preprint. Click to download.

- [SUPPLEMENTARY MATERIAL.docx](#)